Transparency/Opacity of a Solid Target Illuminated by an Ultrahigh-Intensity Laser Pulse

Erik Lefebvre and Guy Bonnaud
Commissariat à l'Energie Atomique, Centre d'Etudes de Limeil-Valenton, 94195 Villeneuve-Saint-Georges, France
(Received 12 August 1994)

By means of one-dimensional particle-in-cell simulations of an ultraintense electromagnetic wave normally incident on an overdense plasma, the transition from a regime of wave reflection to one of penetration is observed, when laser irradiance is increased. Both cases display Doppler-redshifted backscattered light originating from a moving surface. The irradiance threshold for the transition is given as a function of electron density. The energy reflected and the kinetic energies in both electrons and ions are provided.

PACS numbers: 52.40.Nk, 52.35.Nx, 52.60.+h

For the past several years, electromagnetic irradiances above 10^{18} W/cm^2 have been achieved by focusing the picosecond light pulses delivered by compact multiterawatt lasers operating at micrometer wavelength [1]. The associated electric field, which is higher than the electric field existing in the Bohr atom, can then instantaneously transform the matter into a plasma. Moreover, it lets the free electrons quiver with relativistic momentum; the latter, normalized to $m_e c$, is indeed written as $a_0 = 0.85(I_0\lambda_0^2/10^{18})^{1/2}$, where m_e is the electron mass, c is the light velocity in vacuum, λ_0 is the laser wavelength in units of μm, and I_0 is the laser irradiance in units of W/cm^2. The irradiation of a solid target gives rise to high-density free electrons that cannot thermally expand because of the short duration of the laser pulse: The light cannot then deeply penetrate the plasma and interacts only with the sharply edged irradiated plasma surface, at least in cases where $a_0 \ll 1$ (contrasting with the inertial confinement fusion context, where the laser beam propagates in large plasma volumes). It has been predicted that high irradiances, by increasing the inertial electron mass and hence decreasing the effective plasma frequency, will allow a laser to penetrate a "classically opaque" plasma [2–6]: Evidence of this transformation from surface to volume laser-plasma interaction is the present challenge.

In the standard view of laser-plasma interaction, a laser wave with wavelength λ_0 that impinges on a plasma with electron density above $n_c = 10^{21}/\lambda_0^2$ in units of cm^{-3} is partially reflected and partially absorbed by the so-called normal skin effect, resulting from the electron-ion collisions inside the wave penetration depth $c/\sqrt{\omega_{pe}^2 - \omega_0^2}$; ω_{pe} and ω_0 denote the electron plasma frequency and the incident radial frequency, respectively. High electron quiver velocities result in reduced collisions and the anomalous skin effect. Particle-in-cell (PIC) simulations have clearly exhibited collisionless absorption via kinetic effects: resonant absorption and vacuum screening effect for oblique incidence [7], magnetic force $\mathbf{j} \times \mathbf{B}$ [8] for normal incidence generates fast electron bursts entering the solid target. More recent PIC simulations revealed hydrodynamic scenarios, namely, plasma pushing, hole boring [9], and electrostatic shock [10]. Nevertheless, these PIC results neither confirmed nor denied the speculations of the nineteen-seventies, which were based on analytical work, as to the capability of the laser wave to directly penetrate an overdense plasma ($n_e > n_c$). The features of both propagative and standing modes in an infinite-length uniform plasma with fixed ions have been essentially described [2–5] and a few papers have discussed the case of an inhomogeneous plasma [4,5]. Yet no one has considered the unsteady and kinetic aspects of the interaction and the ion mobility influence on the overcritical propagation.

This Letter reports results from $1\frac{1}{2}$D relativistic PIC simulations that evidence a transition between an opacity regime (OR) and a transparency regime (TR), respectively, characterized by the absence or the propagation of the laser wave inside the plasma. We simulated a linearly polarized electromagnetic wave impinging, at normal incidence, on a collisionless, slightly overdense plasma ($1 < n_e/n_c < 10$). We essentially considered the academic case of a homogeneous plasma irradiated by a constant laser amplitude with a sharp front edge, but also report on a linear density ramp impinged on by either a sharp front or a more realistic bell-shaped laser pulse. The latter was modeled by the energy time envelope $f(0 < t < \tau) = \sin^2(\pi t/\tau)$ and $f(t > \tau) = 0$ with $\tau = 377\omega_0^{-1}$, corresponding to a 100 fs FWHM pulse for 1 μm light. The simulations were performed using the code EUTERPE, with singly ionized mobile ions with mass $m_i = 1836m_e$, unless otherwise specified. The plasma is assumed to be electrically neutral, with an initial temperature of 1 keV. Throughout this letter, we will use $c = 1$.

The differences between OR and TR are best illustrated by the electron trajectories displayed in Fig. 1 for (a) OR and (b) TR at density $n_e/n_c = 2$. In the first case, the laser wave does not penetrate the plasma but pushes its surface, resulting in a large density increase and a laser reflectivity $R \approx 1$. In contrast, the plasma edge remains nearly stationary in the second case, while the laser propagates deeper and deeper in the target, setting the electrons in violent motion. Both pictures show a surface recoiling at steady velocity. When irradiance is increased,

 0031-9007/95/74(11)/2002(4)$06.00

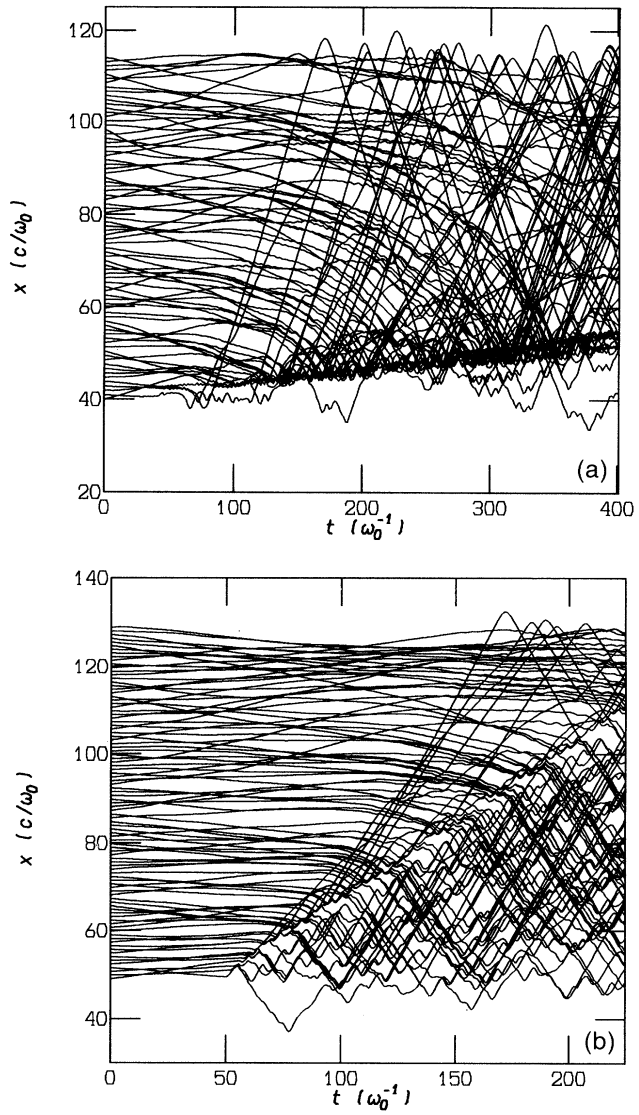

FIG. 1. Electron trajectories for $n_e/n_c = 2$, $m_i/m_e = 1836$, and $a_0 = 2$ (a) or $a_0 = 4$ (b).

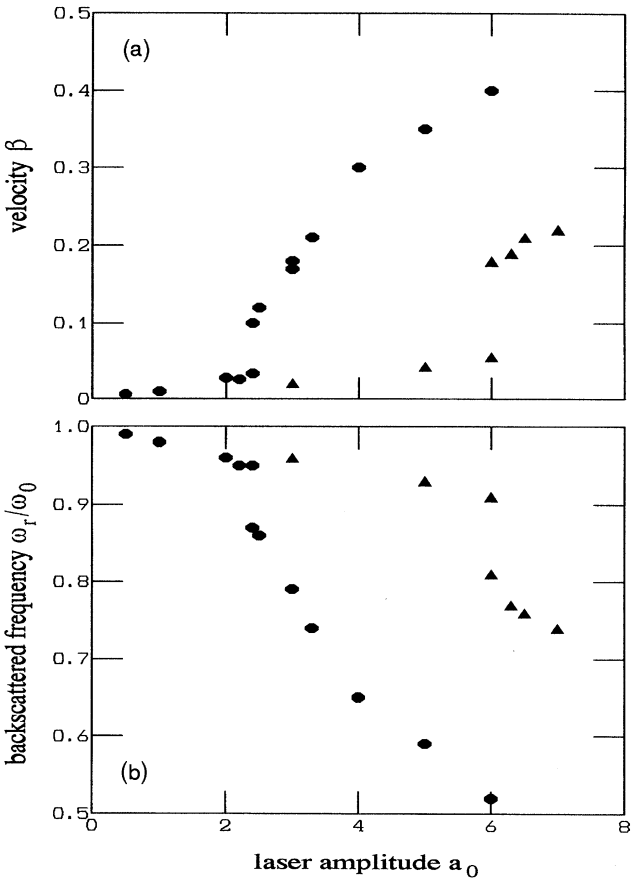

FIG. 2. (a) Velocity of the interface (in units of c) and (b) frequency of the reflected light (in units of ω_0) as a function of the laser amplitude a_0, for $m_i/m_e = 1836$ and $n_e/n_c = 2$ (●) or 4 (▲).

this velocity β exhibits the following features [Fig. 2(a)]: (1) a slow linear increase corresponding to OR, (2) a jump for a critical laser strength a_{0c} (that increases with n_e), and (3) a rapid increase in TR. The frequency ω_r of the light reflected by the plasma displays opposite trends [Fig. 2(b)].

The critical laser amplitude a_{0c} at which the transition between OR and TR occurs can be determined from the β or ω_r plots, but more precisely from the electron trajectories. Indeed, near a_{0c}, the transient penetration of the laser wave can be observed, during which the ions are nearly immobile. Then an ion shock forms, which fully reflects the laser wave (OR). In such cases, two values of β and ω_r are provided. We plot in Fig. 3 the smallest laser irradiance (located with a 5% half-width error for each density) that allows sustained propagation of a square laser pulse within a uniform plasma (for $100\omega_0^{-1}$ at least). For fixed ions and fluid electrons, earlier papers [3,4] estimated this critical strength to be $a_{0\text{th}} = (\pi/2)n_e/n_c$. Our results for immobile ions (noted $a_{0\infty}$ and depicted by stars on Fig. 3) are clearly lower, stressing the importance of kinetic effects in that regime. On the other hand, when ion motion is allowed (squares in Fig. 3), the critical threshold is raised and varies approximately as $a_{0c} = 1.65(n_e/n_c - 0.5)$. At field strengths between $a_{0\infty}$ and a_{0c}, the space charge potential causes the ion density profile to steepen after some delay, preventing deeper propagation of the laser wave.

For the sake of completeness, a few simulations were performed with an inhomogeneous plasma consisting in a long linear density ramp ($n_e = 0$ to $4n_c$ over a distance of $240c/\omega_0$). For each simulated laser irradiance, we measured the maximum initial density that the laser wave could reach. The results are plotted in Fig. 3 with triangles and circles for sharp-edged and bell-like

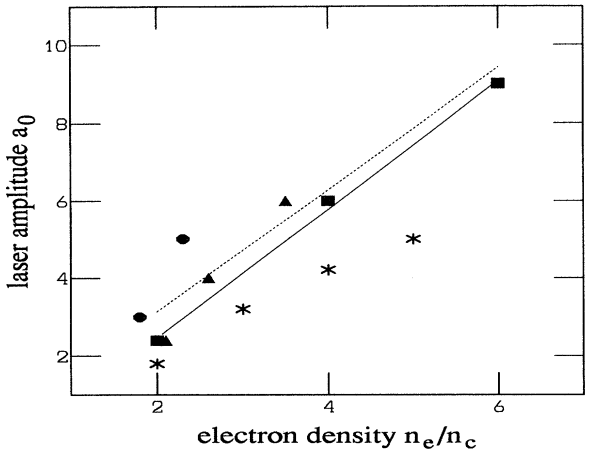

FIG. 3. Irradiance threshold for the penetration/reflection of the laser wave as a function of electron density: continuous wave with a sharp front on a homogenous plasma with $m_i/m_e = \infty$ (*) or $m_i/m_e = 1836$ (■), and continuous wave with a sharp front (▲) or bell-shaped pulse (●) on a linear plasma density ramp with $m_i/m_e = 1836$. Analytical prediction $a_{0\text{th}}$ (dotted line) and numerical fit (solid line).

laser pulses, respectively. We observe that "squares" and triangles" lie very close together, proving that the linear density ramp does not notably alter the penetration process. The bell-shaped pulses give somewhat different results, with maximum densities definitively smaller than for continuous wave pulses. This is no surprise: Due to the long density gradient and the moderate propagation velocity, the pulse needs to be sustained to penetrate to maximum depth. Finally, we note in these cases that the transverse kinetic energy reaches a maximum and then decreases as the pulse ebbs, while the longitudinal kinetic energy keeps increasing until the end of the run.

So far, simulations had been limited to OR [8–10]. Wilks *et al.* [9] obtained the recession velocity of the target by balancing the photon and ion pressure on each side of its surface, assuming total reflection: $\beta_W = a_0[\frac{1}{2}(n_c/n_e)(m_e/m_i)]^{1/2}$. This formula is usually an acceptable approximation; however, in simulations with "light" ions ($m_i/m_e = 100$), we measure velocities much lower than β_W. In this case, pressure arising from hot electron generation at the interface can no longer be neglected. By balancing the energy lost by the laser with that carried away by suprathermal electrons, we can evaluate their contribution to total pressure and deduce an improved expression $\beta_{\text{OR}} = a_0[R/2(n_c/n_e)(m_e/m_i)]^{1/2}$, which is more in line with our simulation results. In OR, the backscattered frequency is simply deduced from β_{OR} by the usual Doppler formula

$$\omega_r = \omega_0 \frac{1 - \beta_{\text{OR}}}{1 + \beta_{\text{OR}}}. \tag{1}$$

In passing, we performed fluid simulations in the same conditions, by means of a recently designed code that solves the relativistic cold hydrodynamic equations for electrons and ions, coupled to Maxwell equations. These simulations always yielded a velocity close to β_W, stressing again the importance of the kinetic effects in PIC simulations (suprathermal electron generation).

Interpretation of the TR data is less straightforward. Our basic hypothesis is that the wave is once again reflected on a moving surface. This surface, which propagates in the plasma at steady velocity β_{TR}, is the place where the wave couples to cold electrons. In the midst of the pulse, the plasma supports two counterpropagating longitudinal-plus-transverse waves of large amplitudes. Assuming that total reflection occurs in the moving surface's frame of reference leads to relations between the incident and reflected wave vectors and frequencies. Then, since the phase velocity v_ϕ of the incident wave is no longer c, the analog to Eq. (1) is derived in a way similar to that used in [11],

$$\frac{\omega_r}{\omega_0} = 1 - 2\beta_{\text{TR}} \frac{1/v_\phi - \beta_{\text{TR}}}{1 - \beta_{\text{TR}}^2}, \tag{2}$$

in good agreement with our simulation results. This attests that reflection does indeed originate from the moving surface and is not a volume reflection, as would take place in Raman scattering. Moreover, the incident and reflected waves in the plasma are only slightly superluminous; if we neglect the reflected wave, the dispersion relation then reads [2]

$$v_\phi^2 = 1 + \frac{\omega_p^2/\omega_0^2}{\sqrt{1 + a_0^2/2}}. \tag{3}$$

The measured phase velocities lie at maximum 10% below those predicted by Eq. (3); this discrepancy probably results from the enhanced lowering of the effective plasma frequency caused by the reflected wave. In Eq. (3), we used a_0 as the field amplitude in the plasma, since no noticeable swelling of the wave was observed.

At the front edge of the pulse, an electron is violently set in motion by the longitudinal ponderomotive force. But the ambipolar field strongly limits its excursion and gives rise to the oscillations depicted in Fig. 1(b), hence, causing the oscillations of the reflecting surface; indeed, its steady drift with velocity β_{TR} results from a succession of elementary recesses, each with amplitude δx and duration δt (in units of c/ω_0 and ω_0^{-1}). Since the ponderomotive force varies at twice the laser frequency, two successive oscillations of the surface will be dephased by the amount

$$\delta t - \delta x/v_\phi = \delta x(1/\beta_{\text{TR}} - 1/v_\phi) = \pi. \tag{4}$$

Since the wave and longitudinal motion frequencies are of the same order, an analytical description of these phenomena is quite involved, hence requiring numerical simulation. If we assume that the interface behavior is reducible to that of a single electron, the maximum

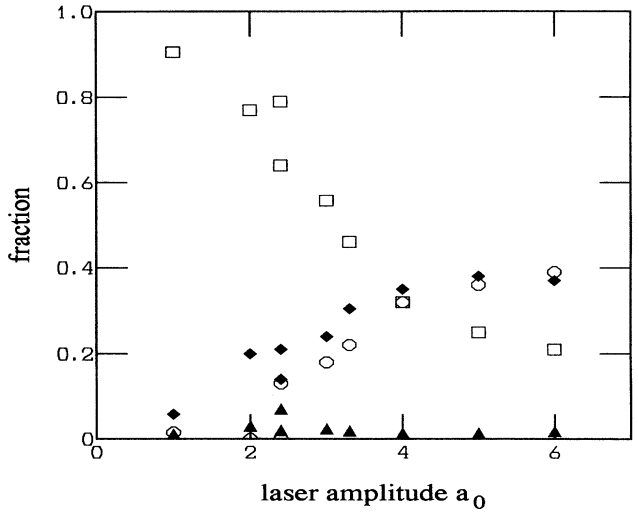

FIG. 4. Reflection rate (□), electromagnetic energy (○), kinetic energies of electrons (◆), and ions (▲), referred to the laser power, as a function of the laser amplitude a_0, for $n_e/n_c = 2$. The laser wave is continuous with a sharp front.

displacement δx can then be calculated by solving the Lorentz force equation for an electron under the action of an electromagnetic wave of phase velocity v_ϕ and a harmonic longitudinal restoring field [12]. Under this drastic assumption, the values of the reflected wave frequency ω_r that are obtained when simultaneously solving Eqs. (2)–(4) for each TR simulation lie within 20% to those observed.

Our last point concerns how the incident energy is converted into wave and kinetic energies. At the end of each simulation, the average increase of the electromagnetic and kinetic energies in the computational box, as well as the electromagnetic energy leaving it, are computed on several laser periods (Fig. 4). Low reflection coefficients are obtained at high intensity (≈25%). Electromagnetic energy is low in OR (since the wave does not enter the plasma), but it becomes comparable to electron kinetic energy in TR. The electromagnetic energy is essentially transverse, while the largest contribution to electron energy stems from longitudinal motion. The ion energy increases in OR and decreases in TR, peaking at 7% around a_{0c}. In OR, however, energy is carried by a few hot ions produced at the interface, while in TR it results from the slight momentum transferred to each ion as the pulse passes by.

In conclusion, the light reflected by a plasma reveals a transition between opacity and transparency when light irradiance is increased. The threshold was clearly identified as a function of electron density and ion mass, and a mechanism for the transparency regime was proposed. This regime can be tested experimentally on solid targets that have been slightly expanded by a laser prepulse in order to work on small plasma volumes between 0 and a few critical densities.

The authors wish to thank P. Audebert, J. Delettrez, J.-P. Geindre, J.-C. Gauthier, and J.-M. Rax for many stimulating discussions and are grateful to F. Bouchut who conceived the algorithms used in the hydro-Maxwell code and to S. Dussy who tested this code.

[1] P. Maine *et al.*, IEEE J. Quantum Electron. **24**, 398 (1988); M. Ferray *et al.*, Opt. Commun. **75**, 278 (1990); M. D. Perry, F. G. Patterson, and J. Weston, Opt. Lett. **15**, 381 (1990); J. P. Watteau *et al.*, Phys. Fluids B **4**, 2217 (1992).

[2] A. I. Akhiezer and R. V. Polovin, Sov. Phys. JETP **3**, 696 (1956).

[3] P. Kaw and J. Dawson, Phys. Fluids **13**, 472 (1970); A. D. Steiger and C. H. Woods, Phys. Rev. A **5**, 1467 (1972); A. Decoster, Phys. Rep. **47**, 285 (1978).

[4] C. Max and F. Perkins, Phys. Rev. Lett. **27**, 1342 (1971).

[5] J. H. Marburger and R. F. Tooper, Phys. Rev. Lett. **35**, 1001 (1975); C. S. Lai, Phys. Rev. Lett. **36**, 966 (1976); F. S. Felber and J. H. Marburger, Phys. Rev. Lett. **36**, 1176 (1976); A. Bourdier and X. Fortin, Phys. Rev. A **20**, 2154 (1979).

[6] N. Tzoar and J. I. Gersten, Phys. Rev. Lett. **28**, 1203 (1972); M. Jain, J. I. Gersten, and N. Tzoar, Phys. Rev. B **10**, 2474 (1974).

[7] F. Brunel, Phys. Rev. Lett. **59**, 52 (1987); G. Bonnaud, P. Gibbon, J. Kindel, and E. Williams, Laser Part. Beams **9**, 339 (1991); P. Gibbon and A. Bell, Phys. Rev. Lett. **68**, 1535 (1992).

[8] W. L. Kruer and K. G. Estabrook, Phys. Fluids **28**, 430 (1985).

[9] S. C. Wilks, W. L. Kruer, M. Tabak, and A. B. Langdon, Phys. Rev. Lett. **69**, 1383 (1992); S. C. Wilks, Phys. Fluids B **5**, 2603 (1993).

[10] J. Denavit, Phys. Rev. Lett. **69**, 3052 (1992).

[11] R. L. Savage, Jr., R. P. Brogle, W. B. Mori, and C. Joshi, IEEE Trans. Plasma Sci. **21**, 5 (1993).

[12] J. N. Bardsley, B. M. Penetrante, and M. H. Mittleman, Phys. Rev. A **40**, 3823 (1989).